Time-gated transillumination and reflection by biological tissues and tissuelike phantoms: simulation versus experiment

K. Michielsen and H. De Raedt

Institute for Theoretical Physics and Materials Science Centre, University of Groningen, Nijenborgh 4, NL-9747 AG Groningen, The Netherlands

N. García

Laboratorio de Física de Sistemas Pequeños y Nanotecnología, Consejo Superior de Investigaciones Científicas, Serrano 144, Madrid E-28006, Spain

Received November 12, 1996; accepted January 27, 1997

A numerical method is presented to solve exactly the time-dependent diffusion equation that describes light transport in turbid media. The simulation takes into account spatial variations of the scattering and absorption factors of the medium and the objects as well as random fluctuations of these quantities. The technique is employed to explore the possibility of locating millimeter-sized objects immersed in turbid media from time-gated measurements of the transmitted or reflected (near-infrared) light. The simulation results for tissuelike phantoms are compared with experimental transillumination data, and excellent agreement is found. Simulations of time-gated reflection experiments indicate that it may be possible to detect objects of 1-mm radius. © 1997 Optical Society of America [S0740-3232(97)03208-0]

Noninvasive diagnostic methods for detection of breast cancer at an early stage are of great importance. A successful screening method should be able to distinguish small tumors from surrounding healthy tissue before metastasis occurs.[1] The ultimate goal is to image millimeter-sized objects in 40–100-mm-thick human tissue. In addition, the potential risk of contracting cancer from repeated exposure to ionizing radiation has increased the interest in noninvasive optical techniques that utilize near-infrared light. Near-infrared light can be used to look at the structure and function of biological systems.[2] In contrast to x-ray mammography, in which in general the incident x rays are scattered at most once, near-infrared light (with wavelengths in the 700–900-nm range) traversing mammalian tissue is scattered strongly but is only weakly absorbed. In mammalian tissue the scattering factor is of the order of 10 cm^{-1}, whereas the absorption factor is of the order of 0.1 cm^{-1}.[3,4]

Light entering a strongly scattering medium that contains one or more small objects (with scattering and/or absorption coefficients different from that of the surrounding medium) arrives at a detector by three different routes:

1. By ballistic transport, in which the photons travel without scattering through the sample to yield a projection of the object(s). These photons arrive first, within a time interval $\tau_1 \approx l/v$, where l is the distance between the source and the detector and v is the velocity of light in the medium. For $l = 6$ cm and $v = 220$ km/s, $\tau_1 \approx 300$ ps.
2. By snakelike paths, in which the photons rattle around the ballistic trajectories, experience a little scattering, and arrive at the detector somewhat later (picosecond time scale). With short (picosecond) pulses and short-time-gated detectors, the ballistic and snakelike, quasi-ballistic photons can be used for direct imaging of the objects.[5–8] Picosecond time-scale imaging techniques have been used to detect objects immersed in highly scattering media.[5–8] A systematic study of the time-gating technique has shown that it is highly sensitive with respect to spatial variations in the absorption or scattering factors,[6] in particular under conditions that are similar to those of biological systems of interest.[6] Recent experiments have shown that the spatial resolution of the time-gating technique can also be obtained with the absorption method.[9] As the signal at the detector contains only an exponentially small fraction of the number of photons in the light pulse emitted by the source, the signal-to-noise ratio is low. In addition, the intensity of these photons decreases exponentially with l, effectively limiting the tissue sample size.
3. By diffusion, in which the photons are scattered many times before they reach the detector. The main problem of imaging with diffuse light stems from the overwhelming scatter of light.

Amplitude-modulated light injected into a scattering medium generates diffusive light-intensity waves.[10] These waves have been shown to behave, in many respects, as propagating waves.[10–16] Inverse scattering techniques in combination with perturbation schemes have been employed to compute spatial variations in the absorption factor $\mu_a(\mathbf{r})$ and the diffusion coefficient $D(r)$ (and hence the location of the objects) from knowledge of the phase and amplitude of these waves at various source

and detector positions.[17] Recently the reconstruction from experimental data of two 10-mm-diameter perfectly absorbing spheres immersed in Intralipid was demonstrated.[17] The diffusive character of the light transport through turbid media usually prohibits the direct detection of weakly absorbing objects hidden in the medium by direct continuous-wave measurement of the transmitted or reflected light intensity.[18]

In the diffusive regime, the strong scattering by the medium blurs the variations in the transmitted or reflected light that result from the local (small) variations of the absorption and the diffusion factor caused by an object immersed in the medium.

Most of the light entering a turbid medium (possibly containing one or more small objects with scattering and/or absorption factors different from those of the medium) is scattered many times before it reaches the detector. For weakly absorbing media the propagation of these photons is, to a good approximation, described by the time-dependent diffusion equation[19–21] (TDDE)

$$\frac{\partial I(\mathbf{r}, t)}{\partial t} = \nabla \cdot D(\mathbf{r})\nabla I(\mathbf{r}, t) - v\mu_a(\mathbf{r})I(\mathbf{r}, t) + S(\mathbf{r}, t), \tag{1}$$

where $I(\mathbf{r}, t)$ is the intensity of light at a point $\mathbf{r}$ and at time t, $D(\mathbf{r}) = v/3[\mu_s'(\mathbf{r}) + \mu_a(\mathbf{r})]$ is the diffusion coefficient, $\mu_s'(\mathbf{r})$ is the reduced scattering factor, and $\mu_a(\mathbf{r})$ denotes the absorption factor. The light source is represented by $S(\mathbf{r}, t)$. The presence of objects is reflected by spatial variations in the absorption factor and/or the reduced scattering factor (and hence also in the diffusion coefficient). In general, both the absorption and the reduced scattering factors will fluctuate randomly around their spatial averages denoted $\bar{\mu}_a$ and $\bar{\mu}_s'$, respectively. For weakly absorbing media, $\bar{\mu}_a \ll \bar{\mu}_s'$.

We have developed software to simulate the time-gating experiments, based on a numerical method to solve TDDE (1). In this paper we demonstrate that the simulation technique yields results that are in excellent agreement with experiment.[6] We then use the technique to determine the conditions under which a small, weakly absorbing object might be detected by measuring the reflected light intensity.

According to Eq. (1) the time evolution of the light intensity at time $t + \tau$ is related to the light intensity at time t through

$$I(\mathbf{r}, t + \tau) = \exp(-\tau H)\left[I(\mathbf{r}, t) + \int_0^\tau d\tau' \times \exp(\tau' H)S(\mathbf{r}, t + \tau')\right], \tag{2}$$

where τ denotes the time step, $H = -\nabla \cdot D(\mathbf{r})\nabla + V(\mathbf{r})$, and $V(\mathbf{r}) = v\mu_a(\mathbf{r})$. From Eq. (2) it follows that all we need to solve the TDDE (1) is an algorithm to compute $\exp(-\tau H)A(\mathbf{r})$ for arbitrary $A(\mathbf{r})$. We have developed an algorithm to compute $\exp(-\tau H)A(\mathbf{r})$ based on the fractal decomposition of matrix exponentials proposed by Suzuki.[22] The algorithm is accurate to second order in the spatial mesh size δ and to fourth order in the time step τ. Conceptually the algorithm is closely related to the one that we developed for the time-dependent Schrödinger equation,[23] and therefore we omit further details here. To mimic realistic situations, the algorithm can deal with spatial variations of the reduced scattering and/or absorption coefficients of the medium (e.g., tissue) or the objects (e.g., tumors) as well as random fluctuations of all these quantities. Furthermore, it has been designed such that it can handle samples of arbitrary shape, a feature that may prove useful for comparing model calculations with *in vivo* experiments.

Our current version of the software solves Eq. (1) in two and three dimensions subject to perfectly reflecting or perfectly absorbing boundary conditions. The intensity of the light transmitted by the sample is collected by detectors located at $\mathbf{r} = (L_x, y, z)$, where L_x denotes the size of the simulation box in the direction of the incident light.[24] The reflected light intensity is recorded at $\mathbf{r} = (0, y, z)$. The light source is placed at $x = 0$ [i.e., $S(\mathbf{r}, t) = 0$ unless $\mathbf{r} = (0, y, z)$]. We carried out simulations using sources of variable size, including the cases of a point source $[S(\mathbf{r}, t) = S_0(t)\delta(x)\delta(y - y_0)\delta(z - z_0)]$ and uniform illumination $[S(\mathbf{r}, t) = S_0(t)\delta(x)]$. At $t = 0$ the source starts to illuminate the system, until $t = t_p$, where it is turned off. Detection of the light intensity starts at $t_d (t_d > t_p)$. Our simulation software allows the detectors to record the instantaneous or the time-integrated light intensity.

To compare with the experimental results of Ref. 6 we made simulations for systems of size 40 mm × 127 mm, with the model parameters taken from Ref. 6. Unless otherwise explicitly stated, the mesh size of the spatial discretization $\delta = 1$ mm, the time step $\tau = 1$ ps, $t_p = 7$ ps, $t_d = 350$ ps, and the speed of light in the medium $v = 22.2$ cm/ns.[25] We verified (by reducing the mesh size and the time step) that the numerical results are, for all practical purposes, exact. The simulation itself is carried out in a manner identical to the procedure used in the time-gating technique.[6] The sample is illuminated uniformly by the pulsed light source. The detector accumulates the light intensity over the interval $t_d < t < t + \Delta t$, where Δt denotes the time gate.

In Fig. 1 we depict our simulation results (dashed curves) and the experimental data (solid curves), which are taken from Fig. 12a of Ref. 6. The medium contains a plastic tube filled with diluted ink, positioned in the center of the sample. In the simulation both the absorption and the scattering factors are allowed to fluctuate randomly within 10% of their values specified in Ref. 6. Our numerical results are in remarkably good agreement with the experimental data. The inset shows the distribution of light inside the sample at $\Delta t = 960$ ps. The object is clearly visible.

Increasing the absorption factor of the diluted ink by a factor of 9 (Fig. 12b of Ref. 6) yields the results shown in Fig. 2. Again, the overall agreement with the experimental[6] data is excellent. Simulation and experimental[6] data for a medium containing bead pairs are shown in Fig. 3. The agreement between experiment and theory is remarkable when one takes into account that no attempt has been made to make a best fit. Figure 4 displays the results for a system containing a plastic tube with ink-tinted milk with the same reduced scatter-

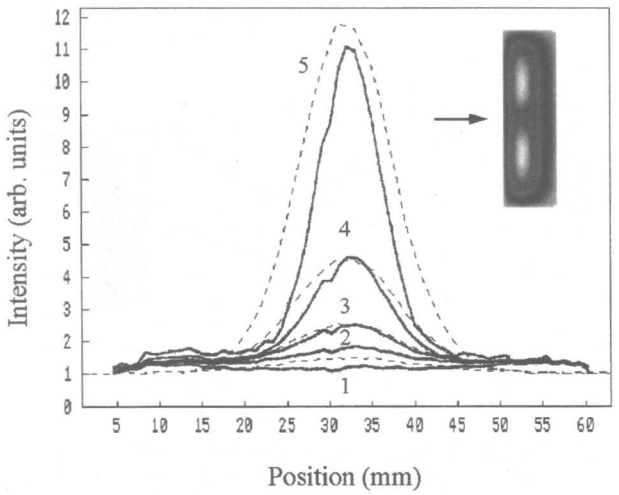

Fig. 1. Comparison of experimental[6] (solid curves) and computer simulation (dashed curves) results for the time-gated transilluminated diffusive light intensity. In experiment and simulation the turbid medium has a reduced scattering factor $\mu_s' = 0.9\ \text{mm}^{-1}$ and an absorption factor $\mu_a < 0.001\ \text{mm}^{-1}$; the absorption factor of the 8-mm-diameter tube is $\mu_a = 0.014\ \text{mm}^{-1}$ (Ref. 6). The reduced scattering factor inside the object is $\mu_s' = 0$. As in Fig. 12(a) of Ref. 6: 1, continuous-wave case (experimental data only); 2, $\Delta t = 960$ ps; 3, $\Delta t = 480$ ps; 4, $\Delta t = 240$ ps; 5, $\Delta t = 30$ ps. The inset shows the light distribution inside the sample for $\Delta t = 960$ ps; the arrow indicates the direction of the incident light. See also Fig. 12(a) of Ref. 6.

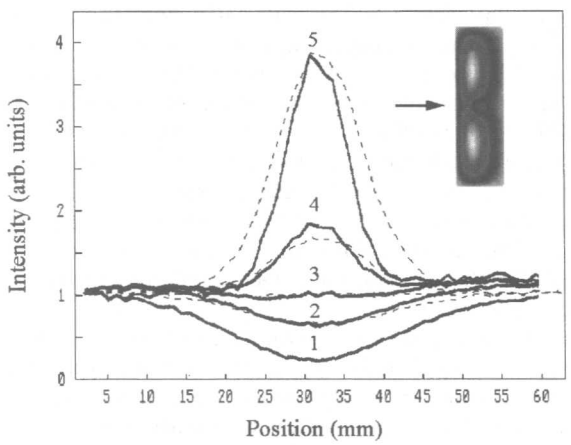

Fig. 2. Same as Fig. 1, except that the absorption factor of the 8-mm-diameter tube is $\mu_a = 0.13\ \text{mm}^{-1}$ (Ref. 6). See also Fig. 12(b) of Ref. 6.

ing factor as the medium but with a different absorption factor. Clearly the simulation data display all the features observed in experiment; in particular, the full width at half-maximum agrees well with the experimental value. Furthermore, our simulation results indicate that the time-gated transilluminated intensity is highly sensitive to the choice of absorption and reduced scattering factors. This is illustrated in Fig. 5, where we show the experimental[6] and simulation results for the same sample as the one used for Fig. 4, except that instead of a difference in the absorption factor of the medium and the object there is a difference only in the scattering factors. Clearly qualitatively similar signals can be obtained for different choices of absorption-scattering factors of the object. Therefore to determine the properties of an object the effect of the reduced scattering and the absorption factors have to be taken into account simultaneously, in agreement with experiment.[6] The above simulation results and others (not shown) demonstrate that our simulation software reproduces all the features observed in the experiments on the tissuelike phantoms reported in Ref. 6.

Our simulation software reproduces, without fitting, the data obtained from time-gated transillumination measurements of turbid media containing relatively large (±8-mm-diameter) objects. Hence it may prove valuable to explore different experimental setups and help to improve methods for data analysis. For instance, it is of interest to know the effect of increasing the size of the sample. In Fig. 6 we show a result of a simulation for a sample of size 63 mm × 63 mm × 63 mm containing a sphere of 4-mm radius positioned at the middle of the sample. The time-gated transmitted intensity contains a clear image of the object, although the image is not as sharp as in the case of a 40-mm thick sample.

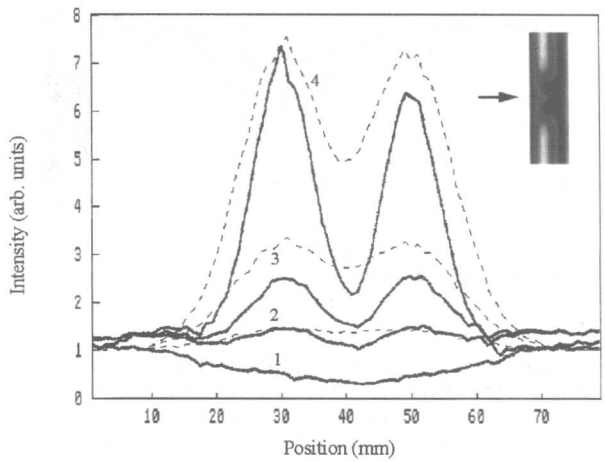

Fig. 3. Same as Fig. 1, except that instead of one there are two 10-mm-diameter objects, separated by 20 mm, with an absorption factor $\mu_a = 0.029\ \text{mm}^{-1}$ (Ref. 6). See also Fig. 13(a) of Ref. 6.

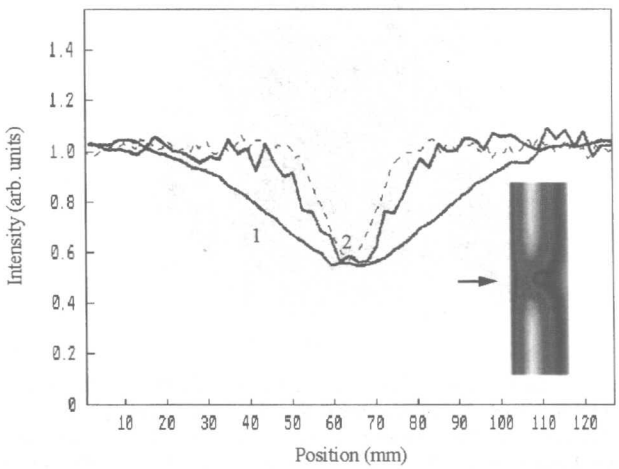

Fig. 4. Same as Fig. 1, except that the turbid medium has a reduced scattering factor $\mu_s' = 0.8\ \text{mm}^{-1}$ and that the absorption and reduced scattering factors of the 8-mm-diameter tube are $\mu_a = 0.1\ \text{mm}^{-1}$ and $\mu_s' = 0.8\ \text{mm}^{-1}$, respectively.[6] See also Fig. 15 of Ref. 6.

An interesting question is to what extent a small object can be detected by a time-gated reflection experiment. In Fig. 7 we show the result of a simulation that gives an indication of the limits of this technique. A 1-mm-radius object is placed 10 mm away from the plane where the light pulse enters the sample. The sample is 63 mm thick and 127 mm wide. In the turbid medium, $\bar{\mu}_s' = 1.1\ \text{mm}^{-1}$ and $\mu_a = 0$. The object has $\mu_s' = 1.1\ \text{mm}^{-1}$ and $\mu_a = 0.11\ \text{mm}^{-1}$, typical values for human tissue.[6,15] From our simulations (results not shown) it follows that to get a clear signal of the object in the reflected intensity it is expedient to increase the time t_d at which the detectors start to record the reflected photons. The results shown in Fig. 7 were obtained for $t_d = 1000$ ps; other parameters such as the timegate Δt are identical to those in Figs. 1–5. We conclude that al-

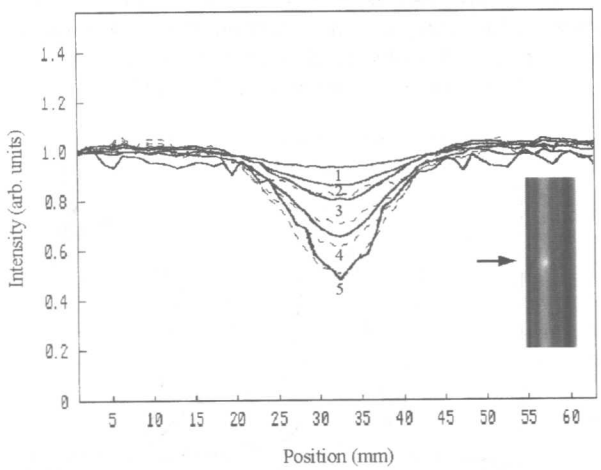

Fig. 5. Same as Fig. 1, except that the turbid medium has a reduced scattering factor $\mu_s' = 0.8\ \text{mm}^{-1}$ and an absorption factor $\mu_a = 0.0005\ \text{mm}^{-1}$ and that the absorption and the scattering factors of the 8-mm-diameter tube are $\mu_a = 0.0005\ \text{mm}^{-1}$ and $\mu_s' = 2.6\ \text{mm}^{-1}$, respectively.[6] See also Fig. 14 of Ref. 6.

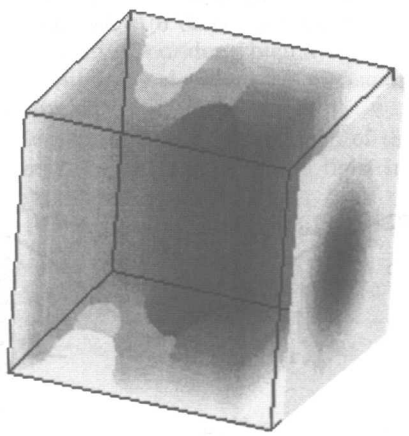

Fig. 6. Simulation of a time-gated transillumination experiment on a turbid medium with a reduced scattering factor $\mu_s' = 1.1\ \text{mm}^{-1}$ and an absorption factor $\mu_a < 0.001\ \text{mm}^{-1}$ containing a 4-mm-radius object with absorption and reduced scattering factors $\mu_a = 0.11\ \text{mm}^{-1}$ and $\mu_s' = 1.1\ \text{mm}^{-1}$, respectively. The dimensions of the sample are 63 mm × 63 mm × 63 mm. The object is located in the middle of the sample. The transmitted intensity for $\Delta t = 1.7$ ns is projected onto the rightmost plane of the sample.

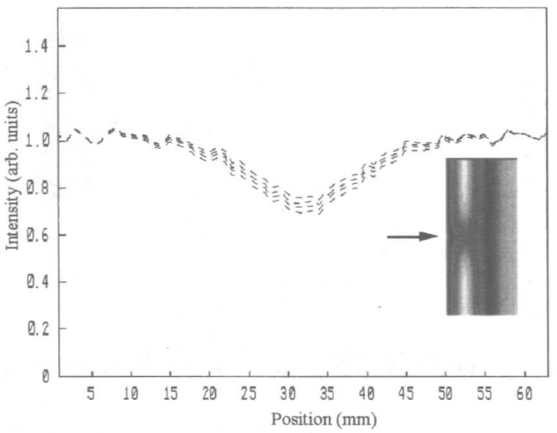

Fig. 7. Simulation of a time-gated reflection experiment on a turbid medium with a reduced scattering factor $\mu_s' = 1.1\ \text{mm}^{-1}$ and an absorption factor $\mu_a < 0.001\ \text{mm}^{-1}$ containing a 1-mm-radius object with absorption and reduced scattering factors $\mu_a = 0.11\ \text{mm}^{-1}$ and $\mu_s' = 1.1\ \text{mm}^{-1}$, respectively. The dimensions of the sample are 63 mm × 127 mm. Curves from bottom to top: $\Delta t = 30$ ps, $\Delta t = 240$ ps, $\Delta t = 480$ ps, $\Delta t = 960$ ps. The inset shows the light distribution inside the sample for $\Delta t = 960$ ps; the arrow indicates the direction of the incident light.

though the object is small (it has a 1-mm radius), it leaves a clear trace in the time-gated reflected intensity. There seems to be no direct relation between the full width at half-maximum and the size of the object. The fingerprint of this small object in the reflected signal disappears if the object is more than 15 mm away from the entrance plane. The possibility of detecting objects, e.g., tumors, of 1-mm radius by reflection measurements offers new possibilities for performing *in vivo* experiments on breasts and brains, with the possible advantage that there is no need to compress or deform the tissue. For both the transillumination and reflection methods, using point sources instead of uniform illumination is much less favorable for the detection of objects hidden in the medium (results not shown).

In conclusion, we have developed software to simulate time-gated transillumination and reflection experiments of light diffusion in turbid media. Our simulation technique reproduces experimental data without the need for fitting parameters. Simulation results for the time-gated reflection technique suggest that, under conditions similar to those of human tissue with tumors, objects of 1-mm radius can be located if they are less than 15 mm away from the surface of the sample.

ACKNOWLEDGMENTS

N. García thanks M. Nieto-Vesperinas for introducing him to the problem of detection of hidden objects. This research is supported by the European Economic Community and Spanish research contracts.

REFERENCES AND NOTES

1. J. C. Hebden, D. J. Hall, M. Firbank, and D. T. Delpy, "Time-resolved optical imaging of a solid tissue-equivalent phantom," Appl. Opt. **34**, 8038–8047 (1995).

2. J. Alper, "Transillumination: looking right through you," Science **261**, 560 (1993).
3. R. Marchesini, A. Bertoni, S. Andreola, E. Melloni, and A. E. Sichirollo, "Extinction and absorption coefficients and scattering phase functions of human tissues *in vitro*," Appl. Opt. **28**, 2318–2324 (1989).
4. A. Kienle, L. Lilge, M. S. Patterson, R. Hibst, R. Steiner, and B. C. Wilson, "Spatially resolved absolute diffuse reflectance measurements for noninvasive determination of the optical scattering and absorption coefficients of biological tissue," Appl. Opt. **35**, 2304–2314 (1996).
5. D. A. Benaron and D. K. Stevenson, "Optical time-of-flight and absorbance imaging of biologic media," Science **259**, 1463–1466 (1993).
6. G. Mitic, J. Kölzer, J. Otto, E. Plies, G. Sölkner, and W. Zinth, "Time-gated transillumination of biological tissues and tissuelike phantoms," Appl. Opt. **33**, 6699–6710 (1994).
7. R. R. Alfano, X. Liang, L. Wang, and P. P. Ho, "Time-resolved imaging of translucent droplets in highly scattering turbid media," Science **264**, 1913–1915 (1994).
8. J. Watson, P. Georges, T. Lépine, B. Alonzi, and A. Brun, "Imaging in diffuse media with ultrafast degenerate optical parametric amplification," Opt. Lett. **20**, 231–233 (1995).
9. D. Contini, H. Liszka, A. Sassaroli, and G. Zaccanti, "Imaging of highly turbid media by the absorption method," Appl. Opt. **35**, 2315–2324 (1996).
10. J. B. Fishkin and E. Gratton, "Propagation of photon-density waves in strongly scattering media containing an absorbing semi-infinite plane bounded by a straight edge," J. Opt. Soc. Am. A **10**, 127–140 (1993).
11. M. A. O'Leary, D. A. Boas, B. Chance, and A. G. Yodh, "Refraction of diffuse photon density waves," Phys. Rev. Lett. **69**, 2658–2661 (1992).
12. D. A. Boas, M. A. O'Leary, B. Chance, and A. G. Yodh, "Scattering and wavelength transduction of diffuse photon density waves," Phys. Rev. E **47**, R2999–R3002 (1993).
13. B. J. Tromberg, L. O. Svaasand, T. T. Tsay, and R. C. Haskell, "Properties of photon density waves in multiple-scattering media," Appl. Opt. **32**, 607–616 (1993).
14. D. A. Boas, M. A. O'Leary, B. Chance, and A. G. Yodh, "Scattering of diffuse photon density waves by spherical inhomogeneities within turbid media: analytic solution and applications," Proc. Natl. Acad. Sci. USA **91**, 4887–4891 (1994).
15. J. M. Schmitt, A. Knüttel, and J. R. Knutson, "Interference of diffusive light waves," J. Opt. Soc. Am. A **9**, 1832–1843 (1992).
16. B. Chance, K. Kang, L. He, J. Wang, and E. M. Sevick, "Highly sensitive object location in tissue models with linear in-phase and anti-phase multi-element optical arrays in one and two dimensions," Proc. Natl. Acad. Sci. USA **90**, 3423–3427 (1993).
17. M. A. O'Leary, D. A. Boas, B. Chance, and A. G. Yodh, "Experimental images of heterogeneous turbid media by frequency-domain diffusing-photon tomography," Opt. Lett. **20**, 426–428 (1995).
18. If the scattering factors of the object and the medium differ considerably, direct detection is possible: See P. N. den Outer, Th. M. Nieuwenhuizen, and A. Lagendijk, "Location of objects in multiple-scattering media," J. Opt. Soc. Am. A **10**, 1209–1218 (1993).
19. A. Ishimaru, *Wave Propagation and Scattering in Random Media* (Academic, New York, 1978).
20. H. C. van de Hulst, *Multiple Light Scattering* (Academic, New York, 1980).
21. A. Yodh and B. Chance, "Spectroscopy and imaging with diffusing light," Phys. Today **48**(3), 34–40 (1995).
22. M. Suzuki, "General theory of fractal path integrals with applications to many-body theories and statistical physics," J. Math. Phys. (N.Y.) **32**, 400–407 (1991).
23. H. De Raedt and K. Michielsen, "Algorithm to solve the time-dependent Schrödinger equation for a charged particle in an inhomogeneous magnetic field: application to the Aharonov–Bohm effect," Comput. Phys. **8**, 600–607 (1994).
24. For the present purpose we employ rectangular boxes, but the algorithm that we use can be modified to handle volumes of arbitrary shape.
25. In the TDDE the speed of light v sets only the time scale. To rescale the results presented in this paper to the case in which the speed of light in the medium is v', multiply all times by v/v'.